Domain Wall Renormalization Group Approach to the 2d Ising Model with External Magnetic Field (Applications of Renormalization Group Methods in Mathematical Sciences)

AUTHOR(S):

青木, 健一; 藤井, 康弘; 小林, 玉青; 佐藤, 大輔; 富田, 洋

数理解析研究所講究録
第1904巻 2014年 13-30

Domain Wall Renormalization Group Approach to the 2d Ising Model with External Magnetic Field

Ken-Ichi Aoki,[1,*] Yasuhiro Fujii,[1,†] Tamao Kobayashi,[2,‡]
Daisuke Sato[1,§] and Hiroshi Tomita[1,¶]
[1]*Institute for Theoretical Physics, Kanazawa University*
[2]*Department of Liberal Arts, Yonago National College of Technology*

Abstract

We represent the spin configuration of 2-dimensional Ising model by the domain wall configuration defined on the dual link and formulate the domain wall renormalization group (DWRG) according to the tensor network renormalization technique. In this report, DWRG is extended to include the external magnetic field by introducing the oriented domain wall variables. The renormalization group transformation is obtained in 6 dimensional parameter space completely analytically and its eigenvalues around the non-trivial fixed point is calculated to give the magnetic susceptibility exponent.

1 Introduction

The 2-dimensional Ising model is one of the best work benches for non-perturbative renormalization group approach [1], because it has non-trivial spontaneous magnetization and also the Onsager's exact solution as the leading guide. In fact, various Renormalization Group (RG) approaches for the model has been already proposed.

The domain wall renormalization group (DWRG) [5] is a new type of renormalization group method adopting the tensor renormalization group (TRG) [2] technique. TRG has been applied to various models, particularly classical and quantum spin models in 2-dimension [3, 4].

In domain wall representation, there has been a remaining non-trivial problem of how to calculate magnetic exponents. Our aim here is to propose a simple extension of our method [5] to include the external magnetic field.

*e-mail address: aoki@hep.s.kanazawa-u.ac.jp
†e-mail address: y-fujii@hep.s.kanazawa-u.ac.jp
‡e-mail address: kobayasi@yonago-k.ac.jp
§e-mail address: satodai@hep.s.kanazawa-u.ac.jp
¶e-mail address: h_tomita@hep.s.kanazawa-u.ac.jp

2 Domain Wall Representation

Domain walls are the boundary of spin up or down domains. The domain wall variables are best put on the dual links defined in Fig.1, where the solid lines represent the original square lattice and the dashed lines represent the dual lattice which is also square. The dual links correspond to the boundary of every neighboring spins.

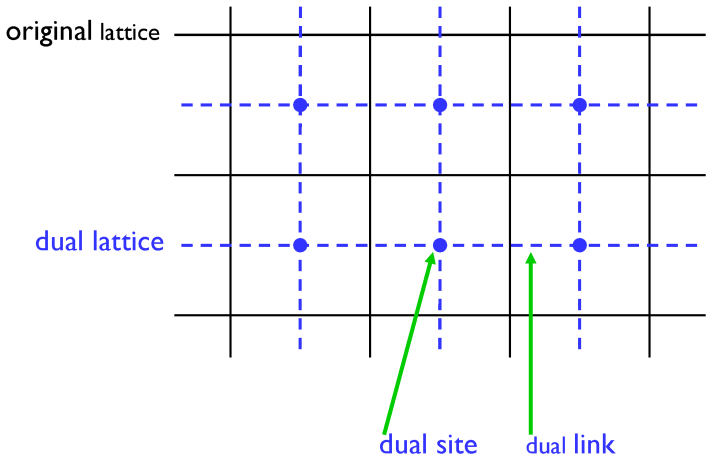

Figure 1: Dual lattice of the 2d square lattice.

The domain wall variables thus reside on the dual links as shown in Fig.2. Spin variables are $\sigma_i = \pm 1$ and domain wall variables are defined by $\alpha_{ij} = \sigma_i \sigma_j$, and it may take two values: $\alpha = +1$ represents no domain wall and $\alpha = -1$ represents the existence of the domain wall.

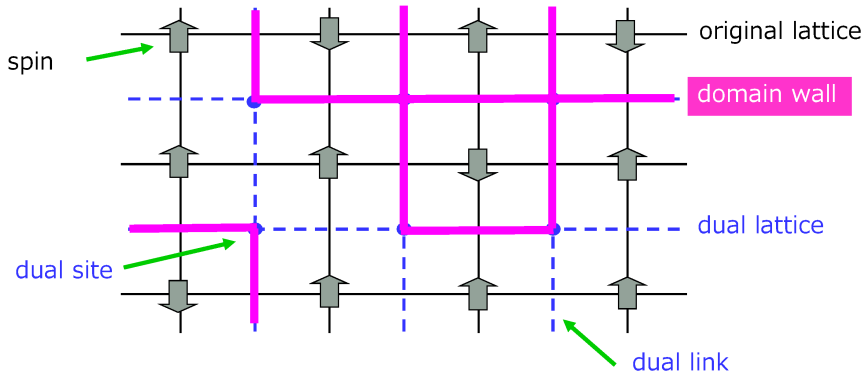

Figure 2: Definition of domain walls.

Any spin configuration can be represented by a domain wall configuration. As shown in Fig.3, the domain wall variables on the four links sharing a single dual site are determined by four spins around it. We regard the final part of Fig.3 as the domain wall vertex defined on the dual site.

However, the correspondence between spins and domain walls are not *one to one*. Tow spin configurations $\{\sigma_i\}$, $\{-\sigma_i\}$ are mapped to the single domain wall configuration $\{\alpha_{ij}\}$

and this is *two to one* mapping. Therefore, although there seems to be no spontaneous symmetry breaking in the domain wall representation, its partition function or the free energy has the exactly same singularities as the original spin partition function.

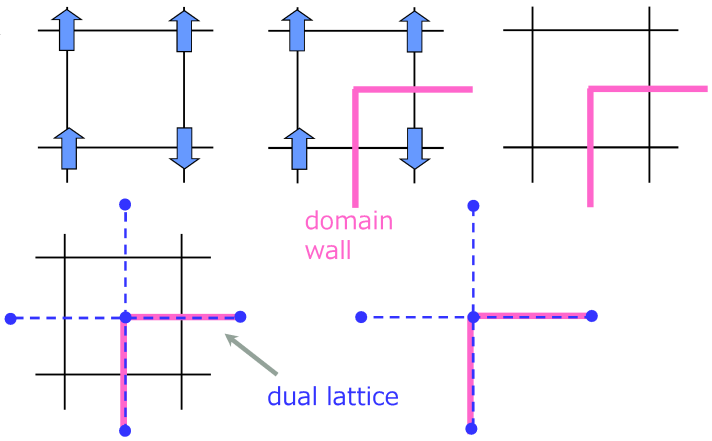

Figure 3: Domain wall representation of spin configuration.

The domain walls constitute the boundary of spin up or down domains, and therefore the domain wall is *conservative* and makes topologically *loop* objects. Then the non-conservative odd vertices as shown in Fig.4 are prohibited.

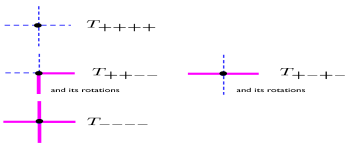

Figure 4: Prohibited non-conservative vertices.

Then we define the vertex tensor at each dual site, which is a function of four domain wall variables around the dual site as shown in Fig.5. Since it has four suffices, it is called the tensor.

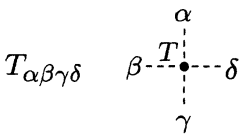

Figure 5: Vertex tensor.

The value of the vertex is determined so that the total product and the total summation with respect to the domain wall variables give the partition function of the original system as shown in Fig.6. The factor 2 at the top represents the *two to one* mapping nature of domain wall configuration versus spin configuration.

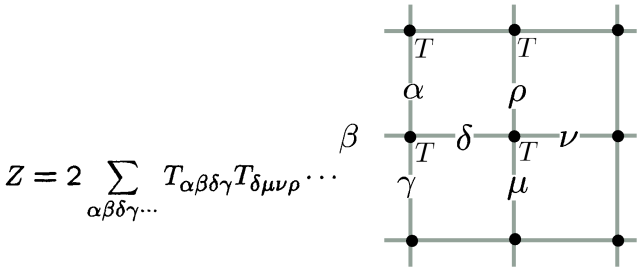

Figure 6: Partition function.

Therefore, the vertex value is proportional to the square root of the local statistical weight of the configuration. In case of non-conservative vertex, the statistical weight must vanish. Then the non-vanishing elements of this $2 \times 2 \times 2 \times 2$ tensor are only 8 elements as shown in Fig.7

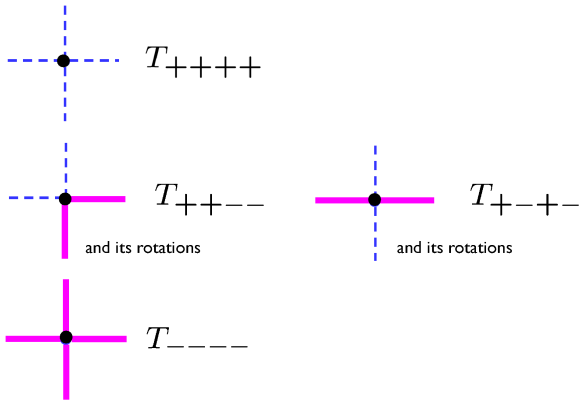

Figure 7: Non-vanishing elements of tensor.

3 Domain wall renormalization group.

In this section we discuss how to define the renormalization group transformation in the domain wall representation, that is, renormalization of its vertex tensor T. The basic strategy to define the renormalization group is flow-charted step by step in Fig.8.

According to this chart, first we define coarse graining of the dual lattice. We define the coarse grained original lattice *a la* Wilson [1], and then the coarse grained dual lattice is automatically defined as in Fig.9.

Note here that the coarse graining of original lattice keeps a half of their sites commonly, while the coarse graining of dual lattice has no common site nor link. In terms of *decimation*, the coarse graining of lattice is obtained by decimation of sites, whereas the coarse graining of dual lattice is obtained by decimation of domains (dual plackets).

Then we define the coarse grained domain status as shown in Fig.10. Note that the decimation of domains here is equivalent to the decimation of spins on the original lattice.

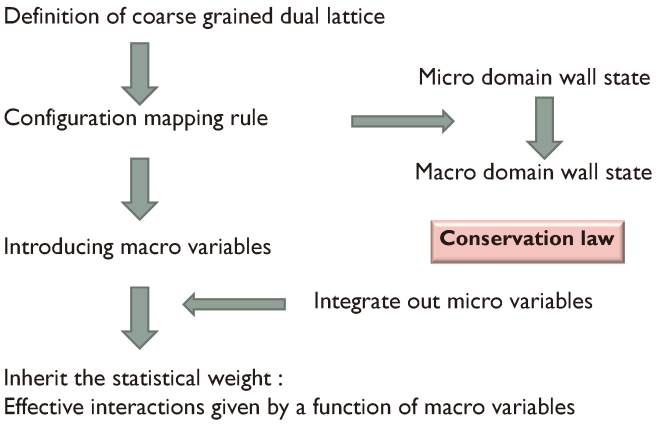

Figure 8: Domain wall renormalization group.

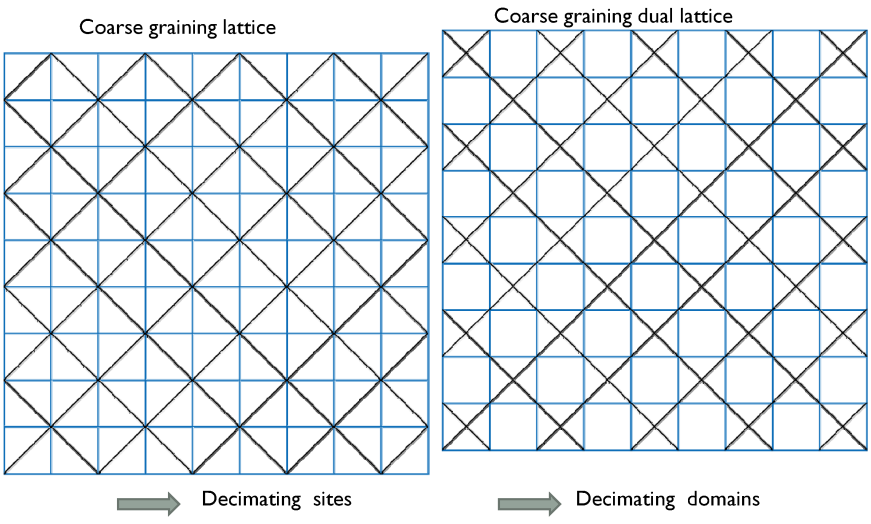

Figure 9: Coarse graining lattice and dual lattice.

The coarse grained domain status is just equal to the micro domain status at the center of it.

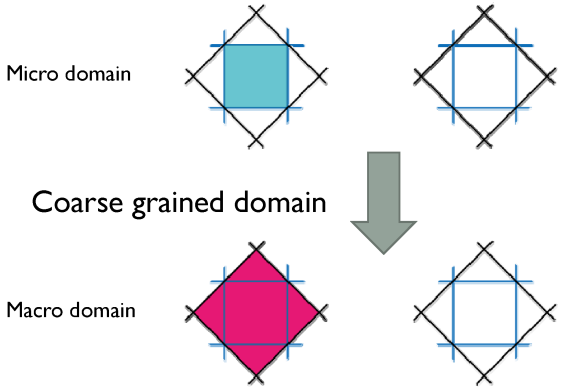

Figure 10: Definition of coarse grained domains.

Next, the coarse grained domain walls are defined by the boundary of the coarse grained domains. Thus we get the mapping function from micro domain wall configuration to the macro domain wall configuration. In Fig.11 we show the mapping function, where the blue dual link denotes the micro domain wall and the red coarse grained dual link denotes the macro coarse grained domain wall. The 4 configurations in the upper row correspond to non-existence of the macro domain wall and those in the lower row correspond to existence of the macro domain wall respectively. It is the *eight to two* reduction mapping and this is *the coarse graining of domain walls*.

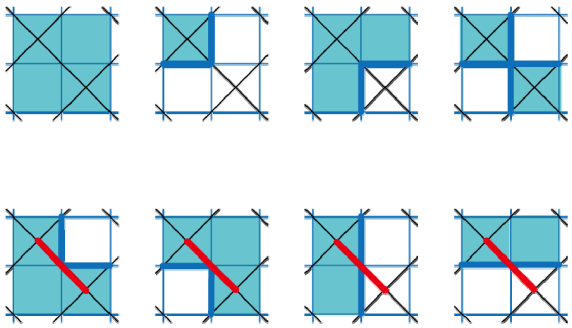

Figure 11: Macro domain walls and the mapping function.

It should be noted here that the macro coarse grained domain walls are boundary of the coarse grained domains, and accordingly the macro domain walls are also conserved by themselves.

An example of the coarse graining of domain walls is shown in Fig.12. The left small island survives the coarse graining whereas the right one disappears.

Now the most non-trivial part comes up. We have defined the domain wall mapping function between micro and macro. Thus the macro domain wall configuration must have some proper statistical weight to be maximally consistent with that given by the micro

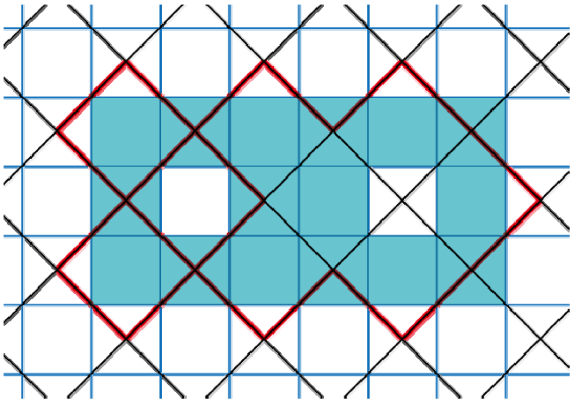

Figure 12: Coarse graining example.

domain wall configuration. And also the macro domain wall weight must be represented by the renormalized tensor vertex. To make this procedure we learn from the tensor network renormalization technique.

First of all, we split the micro domain wall 4-vertex T into a product of 3-vertices S as shown in Fig.13, which is something like transforming the *four-fermi* interactions into a pair of *yukawa* interactions by introducing auxiliary *scalar* fields. This decomposition is performed by the following matrix diagonalization,

$$T = UDV, \tag{1}$$

where tensor T is regarded as a matrix by grouping the domain wall indices as $T_{\{\alpha\beta\}\{\gamma\delta\}}$ and U, V are unitary matrices. The resultant matrix D is a diagonal matrix of singular values λ_M which are all positive semi-definite. Then we can define S as

$$T_{\alpha\beta\gamma\delta} = \sum_M U_{\alpha\beta M}\sqrt{\lambda_M}\sqrt{\lambda_M}V_{M\gamma\delta} = S_{1\alpha\beta M}S_{2\gamma\delta M} \ , \tag{2}$$

$$S_{1\alpha\beta M} = U_{\alpha\beta M}\sqrt{\lambda_M} \ , \ S_{2\gamma\delta M}\sqrt{\lambda_M}V_{M\gamma\delta} \ . \tag{3}$$

Actually our T matrix is a symmetric real matrix and it can be diagonalized by the orthogonal transformation, that is, we have $S_1 = S_2$.

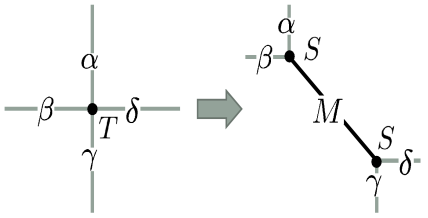

Figure 13: Splitting vertex T.

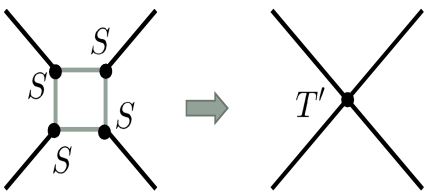

Figure 14: Renormalization of T.

We like to consider the *scalar particle* index M as the macro domain wall variable. Here we have to do some approximation. Since the renormalized domain wall has only two

states naively, while the index M has 4 degrees of freedom to satisfy the above equation. Then we adopt the approximation that only the relatively important channels should be kept, that is, only two indices M are taken among four. This is the approximation we have to do to define the domain wall renormalization group.

Next we integrate out all original domain wall indices $\alpha, \beta, \gamma, \cdots$ and we get the effective weight function of M at each coarse grained (renormalized) dual link, where M is regarded as the renormalized domain wall variable. The effective weight function is written by the renormalized vertex tensor T' defined by

$$T'_{MNKL} = \sum_{\alpha\beta\gamma\delta} S_{\alpha\beta M} S_{\beta\gamma N} S_{\gamma\delta K} S_{\delta\alpha L} \ . \tag{4}$$

This process is understandable as integrating out original *fermion* fields to leave effective interactions among *scalar* fields, and it is graphically expressed in Fig.14.

The global landscape is drawn in Figs.15 and 16. After the renormalization procedure, the renormalized dual lattice has $\sqrt{2}$ times larger spacing. This transformation can be repeated and we have completed to define the domain wall renormalization group in the lowest order approximation.

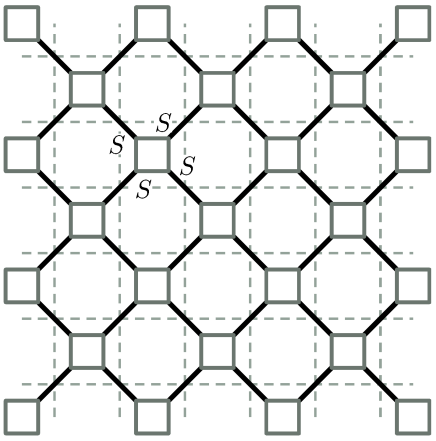

Figure 15: Global landscape 1.

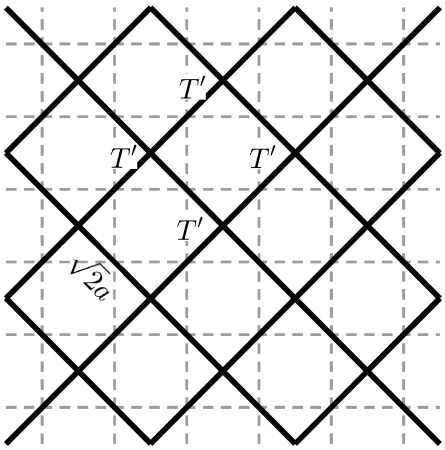

Figure 16: Global landscape 2.

The detailed analysis of this domain wall renormalization group is found in [5]. There, the renormalization transformation is written down completely analytically and it is proved that the physical selection of channels to interpret the renormalized indices as the macro domain wall variables is perfectly consistent with the optimized selection of largest singular values. Also the fixed point structure of the renormalization group flow and the eigenvalues of the renormalization transformation around the fixed point are calculated to give good values compared with the Onsager's exact solution.

4 Introducing the external magnetic field

So far, there is no external field imposed, and no way of calculating magnetic quantities. In this section we propose a simple extension of the domain wall renormalization group to accommodate the external magnetic field.

The domain wall representation is a degenerate description of the spin configurations, that is, it does not discriminate Z_2 inverted spin configurations, $\{\sigma\}$ and $\{-\sigma\}$. To discriminate these Z_2 inversion we introduce orientation of the domain wall as shown in Fig.17. Our rule here is that the up spin domain is on the right hand side of the oriented domain wall when moving along the arrow. Simultaneously we double the no-domain wall state and call them as up domain and down domain as in Fig.18. Now our domain wall variable has four states at every dual link.

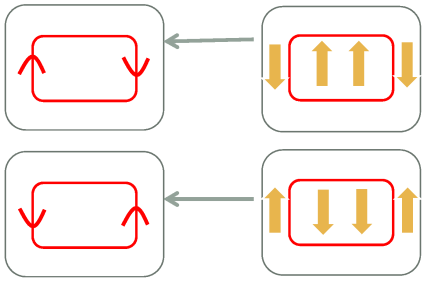

Figure 17: Oriented domain walls.

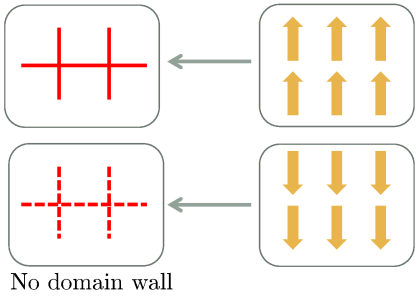

Figure 18: Up domain and down domain.

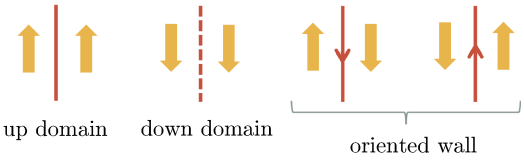

Figure 19: Four domain wall states.

Figure 20: Z_2 symmetry transformation.

The statistical weight is given by,

$$\exp\left(K\sum_{<ij>}\sigma_i\sigma_j + h\sum_i \sigma_i\right) , \tag{5}$$

where $\langle ij\rangle$ means the nearest neighbor pair of spins, K is the coupling constant and h is the external magnetic field. The four states of the domain wall variable on the dual link is diagrammatically expressed as in Fig.19. The Z_2 conjugate transformation is defined for these states as in Fig.20, which is important to understand the symmetry constraint of the vertex tensor and its renormalization transformation.

Now the indices α, β, γ, δ of tensor T takes 4 states each as in Fig.19, and tensor $T_{\alpha\beta\gamma\delta}$ has originally $4^4 = 256$ elements. Only 16 elements are non-vanishing including rotation because of the domain wall conservation law with orientation, which are listed in Fig.21. In Fig.21, the barred variable means Z_2 conjugate, while $a = \bar{a}$, $c = \bar{c}$ are self Z_2 conjugate.

This domain wall representation has 6 dimensional parameter space $\{N,\ \overline{N},\ b,\ \bar{b},\ a,\ c\}$ and *one to one* correspondence to spin interactions $\{C_0,\ K,\ K_D,\ K_4,\ h,\ h_3\}$, whose definition is given by Eq.(6) and Fig.22,

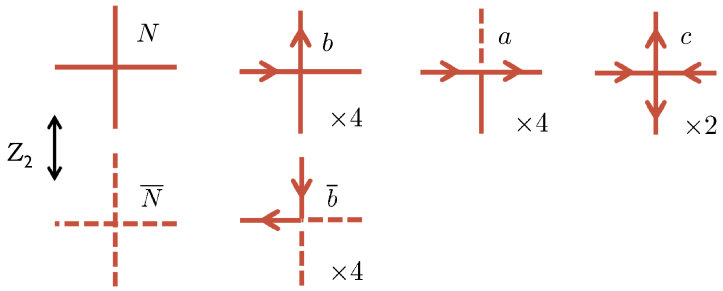

Figure 21: Non-vanishing 16 elements of the vertex tensor.

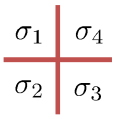

Figure 22: Spin configuration.

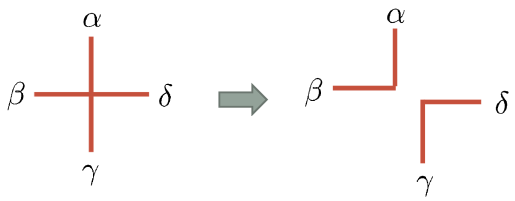

Figure 23: 2-dimensional matrix.

$$\exp\left[C_0 + K(\sigma_1\sigma_2 + \sigma_2\sigma_3 + \sigma_3\sigma_4 + \sigma_4\sigma_1) + K_D(\sigma_1\sigma_3 + \sigma_2\sigma_4) + K_4(\sigma_1\sigma_2\sigma_3\sigma_4)\right.$$
$$\left. + h(\sigma_1 + \sigma_2 + \sigma_3 + \sigma_4) + h_3(\sigma_1\sigma_2\sigma_3 + \sigma_2\sigma_3\sigma_4 + \sigma_3\sigma_4\sigma_1 + \sigma_4\sigma_1\sigma_2)\right] . \quad (6)$$

We use 2-dimensional matrix representation $T_{\{\alpha\beta\}\{\gamma\delta\}}$ of $T_{\alpha\beta\gamma\delta}$ as in Fig.23, and matrix $T_{\{\alpha\beta\}\{\gamma\delta\}}$ is 16×16 dimensional. Actually, non-vanishing indices $\{\alpha\beta\}$ or $\{\gamma\delta\}$ are very much and limited as shown in Fig.24. Only 8 elements are non-vanishing among 16 elements, and therefore $T_{\{\alpha\beta\}\{\gamma\delta\}}$ has only 8×8 non-vanishing block.

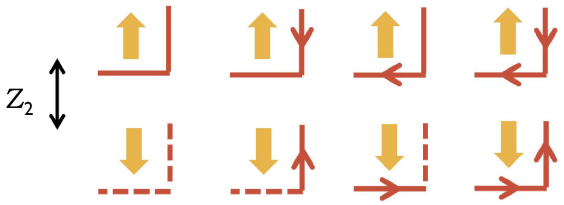

Figure 24: Non-vanishing indices.

Considering the oriented domain wall conservation law, possible combination of indices $\{\alpha\beta\}$ and $\{\gamma\delta\}$ are summarized in Fig.25. Thus the matrix $T_{\{\alpha\beta\}\{\gamma\delta\}}$ is divided into the even section and odd section and their Z_2 conjugate sections. Each section consists of 2×2 structure. Odd section and $\overline{\text{odd}}$ section are also constrained by the rotational symmetry. Accordingly, the total image of $T_{\{\alpha\beta\}\{\gamma\delta\}}$ takes the form shown in Fig.26. The matrix $T_{\{\alpha\beta\}\{\gamma\delta\}}$ is block diagonal consisting of 4 blocks of 2×2 each.

Now we set up the oriented domain wall renormalization group. The renormalized domain wall states are defined by renormalized domain states. Then each sector corresponds to a unique macro domain wall state as shown in Fig.27. To keep the domain

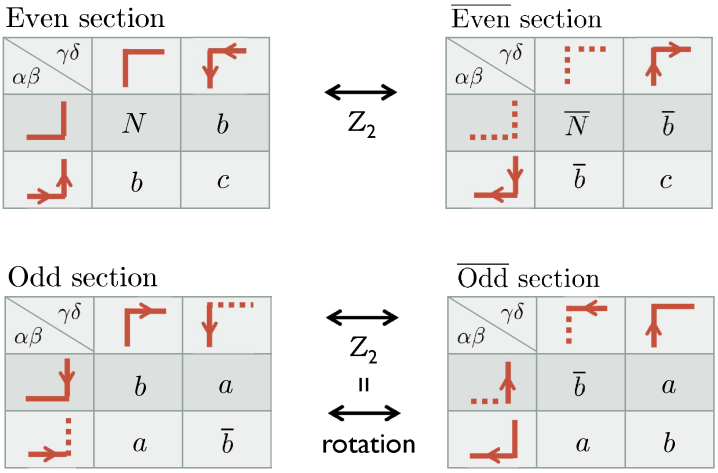

Figure 25: Even and odd section.

wall interpretation through the renormalization procedure, we have to pick up one macro channel each from every section.

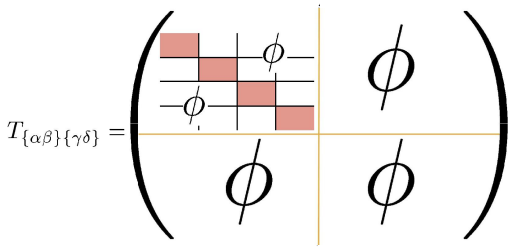

Figure 26: Block diagonal matrix T.

We diagonalize $T_{\{\alpha\beta\}\{\gamma\delta\}}$ as follows. Cosine and sine functions constituting the orthogonal matrices are denoted by c_a, s_a. Diagonalization of even sector is given by,

$$\begin{pmatrix} N & b \\ b & c \end{pmatrix} = \begin{pmatrix} c_1 & -s_1 \\ s_1 & c_1 \end{pmatrix} \begin{pmatrix} \lambda_1 & 0 \\ 0 & \lambda_2 \end{pmatrix} \begin{pmatrix} c_1 & s_1 \\ -s_1 & c_1 \end{pmatrix} . \tag{7}$$

$\overline{\text{Even}}$ section is expressed by using the Z_2 conjugate variables,

$$\begin{pmatrix} \overline{N} & \overline{b} \\ \overline{b} & \overline{c} \end{pmatrix} = \begin{pmatrix} \overline{c_1} & -\overline{s_1} \\ \overline{s_1} & \overline{c_1} \end{pmatrix} \begin{pmatrix} \overline{\lambda_1} & 0 \\ 0 & \overline{\lambda_2} \end{pmatrix} \begin{pmatrix} \overline{c_1} & \overline{s_1} \\ -\overline{s_1} & \overline{c_1} \end{pmatrix} . \tag{8}$$

Odd and $\overline{\text{odd}}$ sections are parametrized by,

$$\begin{pmatrix} b & a \\ a & \overline{b} \end{pmatrix} = \begin{pmatrix} c_2 & -s_2 \\ s_2 & c_2 \end{pmatrix} \begin{pmatrix} \lambda_3 & 0 \\ 0 & \lambda_4 \end{pmatrix} \begin{pmatrix} c_2 & s_2 \\ -s_2 & c_2 \end{pmatrix} , \tag{9}$$

where we adopt the following Z_2 conjugation rules,

$$\overline{\lambda_3} = \lambda_3, \ \overline{c_2} = s_2, \ \overline{s_2} = c_2 . \tag{10}$$

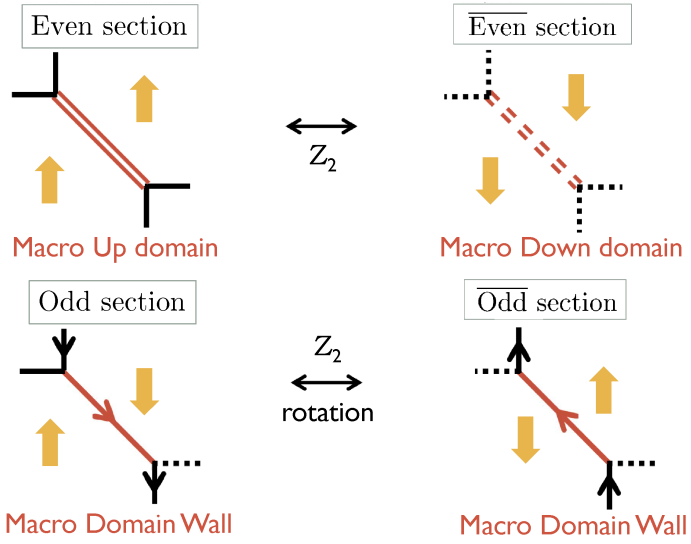

Figure 27: Macro domain wall states.

Here larger eigenvalues (selected channels) in each section are taken to be λ_1, $\overline{\lambda_1}$, λ_3, $\overline{\lambda_3}$, and they are also the 4 largest singular values of all 8 singular values, which assures our physical selection is consistent with the optimized singular value decomposition policy.

The Feynman rules which couples micro and macro domain walls are listed in Fig.28. Domain walls are conserved in total for micro and macro. It should be noted that they are oriented Feynman rules and therefore they are irreversible, that is, the example diagrams at the bottom of Fig.28 do not exist.

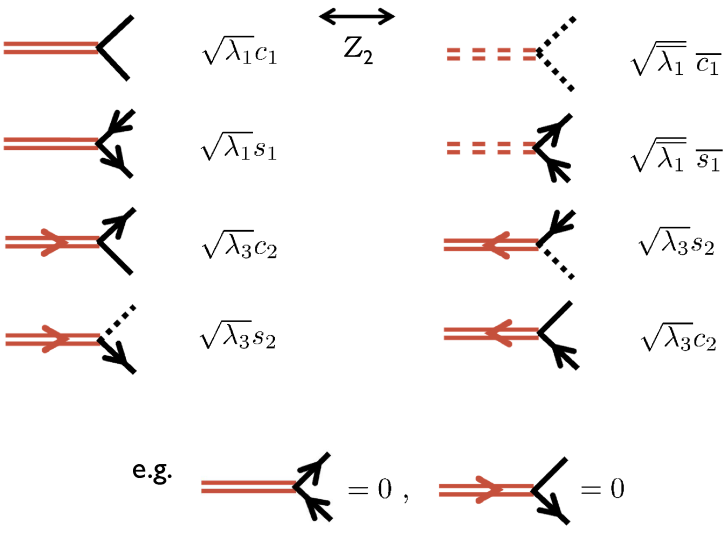

Figure 28: Feynman rules between micro and macro.

Renormalization transformation is carried out by calculating the one-loop diagrams as in Fig.29. Note that all transformation rules are consistent with the Z_2 conjugation.

For example a' and c' keep Z_2 self conjugateness.

From the statistical weight defined in Eq.(5), the physical initial values of these 6 parameters are given by,

$$\begin{aligned} N &= e^{2K+h} \longleftrightarrow \overline{N} = e^{2K-h} , \\ b &= e^{h/2} \longleftrightarrow \bar{b} = e^{-h/2} , \\ a &= 1, \ c = e^{-2K} , \end{aligned} \tag{11}$$

where left and right handed sides of $\leftrightarrow$ are Z_2 conjugate to each other.

Now we write down the renormalization group transformation explicitly and analytically as follows,

$$\begin{aligned} \lambda_1 &= \frac{1}{2}\left(N + C + \sqrt{(N-C)^2 + 4b^2}\right) , \\ \overline{\lambda_1} &= \frac{1}{2}\left(\overline{N} + C + \sqrt{(\overline{N}-C)^2 + 4\bar{b}^2}\right) , \\ \lambda_3 &= \frac{1}{2}\left(b - \bar{b} + \sqrt{(b-\bar{b})^2 + 4a^2}\right) , \\ t_1 &= \frac{1}{b}(\lambda_1 - N) , \quad t_1 = \frac{1}{\bar{b}}(\overline{\lambda_1} - \overline{N}) , \quad t_2 = \frac{\lambda_3 - b}{a} , \\ c_a^2 &= \frac{1}{1+t_a^2} , \quad s_a^2 = 1 - c_a^2 , \quad \text{for } a = \{1, \ \bar{1}, \ 2\} . \end{aligned} \tag{12}$$

Due to the Z_2 conjugate property of the total system, there exists a 4-dimensional subspace of Z_2 invariant space,

$$N = \overline{N}, \ b = \bar{b}, \ a, \ c , \tag{13}$$

in which the renormalization group flows are confined. Therefore this subspace is renormalization group invariant subspace. The renormalization group transformation in this Z_2 invariant subspace is exactly equal to what we have obtained previously [5].

We have to find the non-trivial fixed point to evaluate critical properties of the spontaneous magnetization. Actually, however, there is no fixed point in the transformation in Eq.(12), since the vertex tensor T continues to increase due to the volume effect of the renormalization procedure which compensates the decimation of half of the degrees of freedom at each renormalization step. We will set some normalization condition of T and multiply a constant factor to all elements in T to satisfy it at each renormalization step. This is called the *gauge fixing* since such constant multiplication does not change any physical quantities of density type objects, such as, magnetization per site *etc.*

The position of a fixed point itself depends on the *gauge fixing condition* adopted, called the *gauge* simply. However, the eigenvalues around the fixed point does not depend on the gauge. Here we show a proof of it briefly. We have two gauge fixing conditions, and coordinates on the gauge fixed manifolds are denoted by x and y respectively. There are gauge transformation path (fiber bundle) in the total space on which T is physically equivalent. This gauge transformation defines a relation between x and y,

$$y = g(x), \tag{14}$$

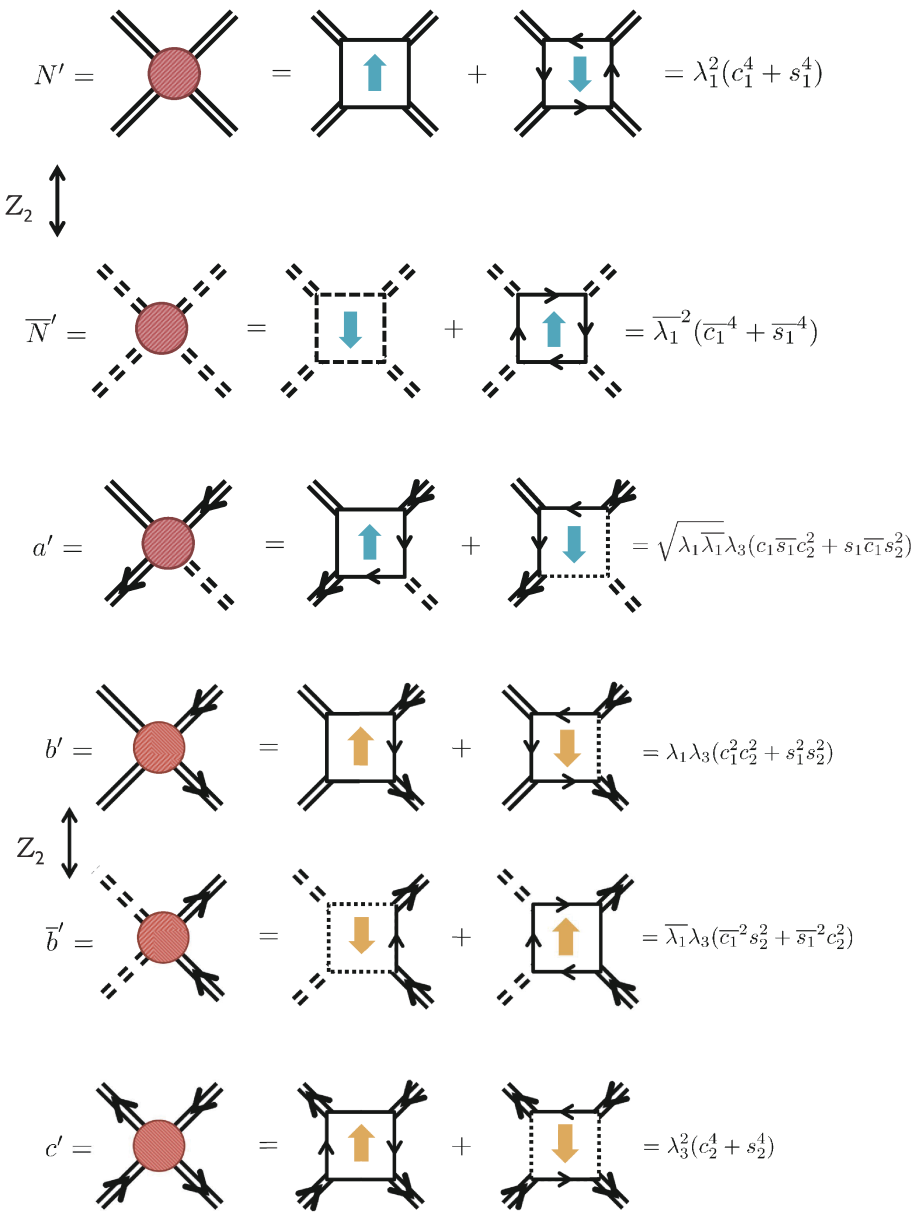

Figure 29: Renormalization transformation.

where g is a non-singular function. Now the renormalization transformation are written as

$$x' = R_1(x) \ , \quad y' = R_2(y), \tag{15}$$

and they have a fixed point at x^* or y^* satisfying,

$$x^* = R_1(x^*) \ , \quad y^* = R_2(y^*) \ , \quad y^* = g(x^*). \tag{16}$$

The eigenvalues for x and y spaces are denoted by λ_1 and λ_2 respectively, and they are calculated to coincide with each other as follows,

$$\begin{aligned} \lambda_1 &= R_1'(x^*) = \frac{d}{dx}[g^{-1}(R_2(g(x^*)))] = g^{-1\prime}(R_2(g(x^*)))R_2'(g(x^*))g'(x^*) \\ &= g^{-1\prime}(y^*)R_2'(y^*)g'(x^*) = R_2'(y^*) = \lambda_2 \end{aligned} \tag{17}$$

After the gauge fixing, the effective dimension of the total parameter space is five. In the Z_2 invariant 3-dimensional subspace we have found a non-trivial fixed point [5]. This fixed point is also a fixed point in the total 5-dimensional space. The eigenvalues around the fixed point consist of three Z_2 even eigenvalues and two Z_2 odd eigenvalues.

We show transformation of variables between $\{C_0,\ K,\ K_D,\ K_4,\ h,\ h_3\}$ and domain representations $\{N,\ \overline{N},\ b,\ \bar{b},\ a,\ c\}$ in Fig.30, where letters in red are contributed by Z_2 odd interactions.

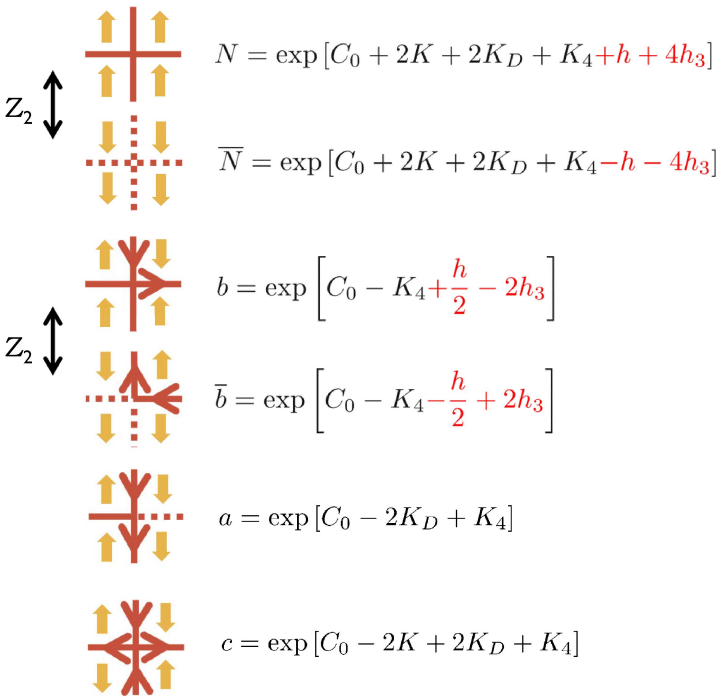

Figure 30: Transformation between spin and domain wall interactions.

The inverse transformation from domain wall interactions $\{N,\ \overline{N},\ b,\ \bar{b},\ a,\ c\}$ to spin

interactions $\{C_0,\ K,\ K_D,\ K_4,\ h,\ h_3\}$ are given by,

$$\begin{aligned} C_0 &= \frac{1}{16}\log\left[N\overline{N}a^4b^4\bar{b}^4c^2\right] , \quad K = \frac{1}{8}\log\left[N\overline{N}/c^2\right] , \\ K_D &= \frac{1}{16}\log\left[N\overline{N}c^2/a^4\right] , \quad K_4 = \frac{1}{16}\log\left[N\overline{N}a^4c^2/b^4\bar{b}^4\right] , \\ h &= \frac{1}{4}\log\left[Nb^2/\overline{N}^2\bar{b}^2\right] , \quad h_3 = \frac{1}{16}\log\left[N\bar{b}^2/\overline{N}^2b^2\right] . \end{aligned} \tag{18}$$

In the actual analysis of the renormalization group flow, we set a *gauge fixing* condition, $C_0 = 0$, that is, the spin independent factor is discarded.

5 Results

The Z_2 even quantities such as the free energy, the specific heat and the correlation length exponent have been reported previously [5]. Here we show Z_2 odd magnetic properties only.

We plot typical high and low temperature flows in terms of the spin interaction parameters in Fig.31 and Fig.32, where n is the number of renormalization steps. In both cases only the single spin magnetic interaction h survives at the infrared (macro) limit, since we have to work with finite correlation length situation. The difference between high and low temperatures is seen by the final enhancement factor of h.

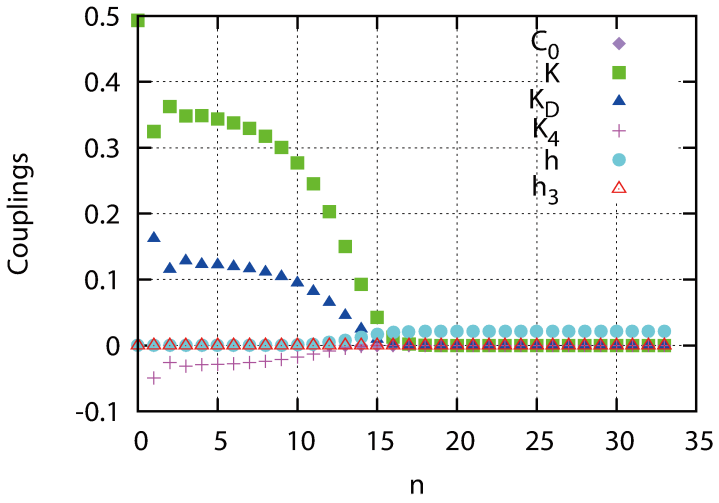

Figure 31: High temperature flow.

In Fig.33, we plotted the magnetization versus the initial nearest neighbor coupling constant ($\alpha \equiv e^{-2K}$) for various initial external magnetic fields. We can see the second order phase transition of the spontaneous magnetization around $\alpha = 0.37036$.

Finally we evaluate renormalization group eigenvalues around the non-trivial fixed point. We have three Z_2-even eigenvalues,

$$\{1.4224,\ -0.2908,\ 0\} , \tag{19}$$

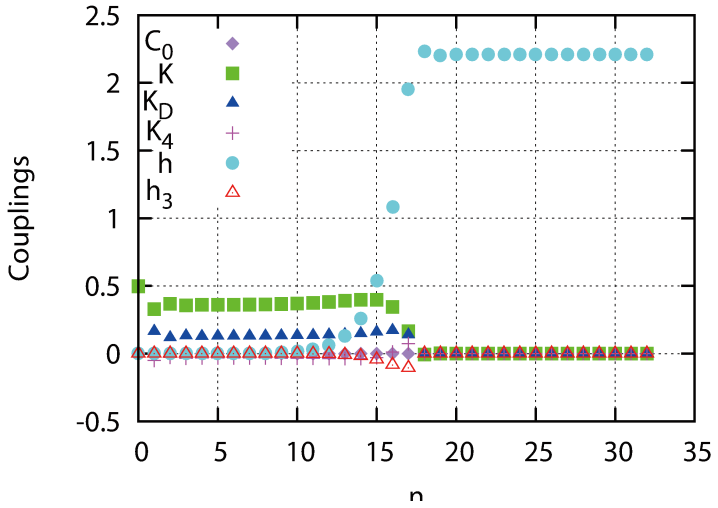

Figure 32: Low temperature flow.

and two Z_2 odd eigenvalues,

$$\{2.0214,\ 1.0547\}\ . \tag{20}$$

The relevant Z_2-even eigenvalue gives the correlation length critical exponent,

$$\nu = \frac{\log\sqrt{2}}{\log 1.4224} = 0.984\ , \tag{21}$$

which looks perfect compared to the exact value of 1. The peculiar zero eigenvalue appears because the renormalization group transformation in the Z_2 even 3-dimensional subspace is actually constrained to be 2-dimensional. This seems an occasional constraint and no physical significance is expected.

As for Z_2-odd eigenvalues, we encounter a serious deficit; there are two relevant operators. So far we have no good idea about how to cure this problem in this lowest order formulation. Some normalization issue owing to the singularity of decimation type renormalization group may be related. If we use the larger eigenvalue to evaluate the magnetic susceptibility exponent,we have

$$\gamma = 2.028\ , \tag{22}$$

which looks not so good compared to the exact value of 7/4.

We have another idea of including the external magnetic field in the dual representation of the domain wall representation. Analysis of this dual renormalization group will be reported elsewhere [6].

Acknowledgments

We thank Yusuke Yoshimura for fruitful and critical discussion and comments, and appreciate very much for inspiring correspondences by Prof. Leo Kadanoff.

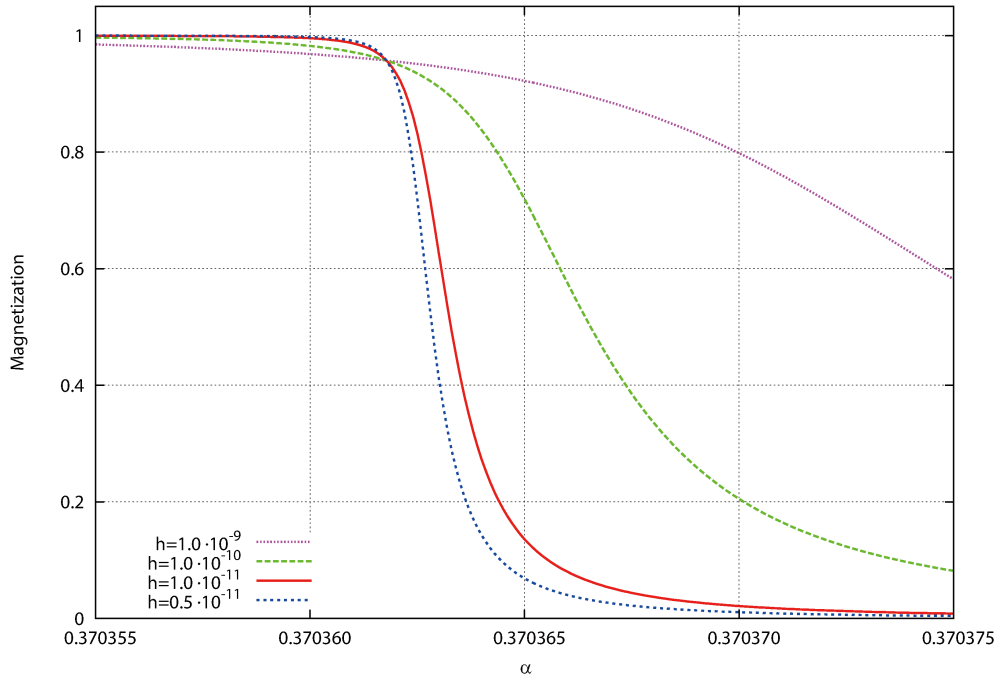

Figure 33: Magnetization versus temperature.

References

[1] L.P. Kadanoff, Physics. **2** (1966) 263.
K. G. Wilson, Rev. Mod. Phys. **47** (1975) 773

[2] M. Levin and C. P. Nave, Phys. Rev. Lett. **99** (2007) 120601.

[3] M. Hinczewski and A. N. Berker, Phys. Rev. E **77** (2008) 011104.

[4] Z.-C. Gu, M. Levin and X.G. Wen, Phys. Rev. B **78** (2008) 205116 and arXiv:0806.3509 [cond-mat.str-el].

[5] K.-I. Aoki, Tamao Kobayashi and H. Tomita, Int.J.M.Phys.B **23** (2009) 3739.

[6] K.-I. Aoki, Yasuhiro Fujii, Tamao Kobayashi, Daisuke Sato, Hiroshi Tomita and Yusuke Yoshimura, in preparation.